Investigating the pygmy dipole resonance using decay

Scheck, M.; Mishev, S.; Ponomarev, V. Yu.; Chapman, R.; Gaffney, L.P.; Gregor, E.T.; Pietralla, N.; Spagnoletti, Pietro; Savran, D.; Simpson, G.S.

Published in:
Physical Review Letters

DOI:
10.1103/PhysRevLett.116.132501

Published: 30/03/2016

Document Version
Publisher's PDF, also known as Version of record

Investigating the Pygmy Dipole Resonance Using β Decay

M. Scheck,[1,2,*] S. Mishev,[3,4] V. Yu. Ponomarev,[5] R. Chapman,[1,2] L. P. Gaffney,[1,2] E. T. Gregor,[1,2] N. Pietralla,[5] P. Spagnoletti,[1,2] D. Savran,[6] and G. S. Simpson[1,2]

[1]*School of Engineering and Computing, University of the West of Scotland, Paisley PA1 2BE, United Kingdom*
[2]*SUPA, Scottish Universities Physics Alliance, Glasgow G12 8QQ, United Kingdom*
[3]*JINR, Joint Institute for Nuclear Research, Dubna 141980, Russia*
[4]*Institute for Advanced Physical Studies, New Bulgarian University, Sofia 1618, Bulgaria*
[5]*Institut für Kernphysik, Technische Universität Darmstadt, D-64289 Darmstadt, Germany*
[6]*ExtreMe Matter Institute EMMI and Research Division, GSI Helmholtzzentrum für Schwerionenforschung, D-64291 Darmstadt, Germany*

(Received 30 October 2015; published 30 March 2016)

In this contribution it is explored whether γ-ray spectroscopy following β decay with high Q values from mother nuclei with low ground-state spin can be exploited as a probe for the pygmy dipole resonance. The suitability of this approach is demonstrated by a comparison between data from photon scattering, $^{136}\mathrm{Xe}(\gamma,\gamma')$, and $^{136}\mathrm{I}$ $[J_0^\pi = (1^-)] \rightarrow {}^{136}\mathrm{Xe}^*$ β-decay data. It is demonstrated that β decay populates 1^- levels associated with the pygmy dipole resonance, but only a fraction of those. The complementary insight into the wave functions probed by β decay is elucidated by calculations within the quasiparticle phonon model. It is demonstrated that β decay dominantly populates complex configurations, which are only weakly excited in inelastic scattering experiments.

DOI: 10.1103/PhysRevLett.116.132501

In the last few decades an additional structure in the $E1$-strength distribution of atomic nuclei has been established near the particle-separation thresholds. It appears as a resonancelike accumulation of 1^- levels on top of the low-energy tail of the isovector giant dipole resonance (GDR) [1] and is denoted as the pygmy dipole resonance (PDR) [2]. While the GDR exhausts 100% or even more of the $E1$ strength predicted by the Thomas-Reiche-Kuhn sum rule, the $E1$ strength of the PDR is typically of the order of a few percent or even less. A detailed survey of experimentally determined $E1$ strengths for nuclei where they have been measured and the method used to extract those are summarized in Ref. [2]. The geometric picture that is most commonly associated with this additional $E1$ strength is an out-of-phase motion of excess neutrons versus an almost isospin-saturated ($N \approx Z$) core. Indeed, transition densities calculated within microscopic models [3], such as the quasiparticle phonon model (QPM) [4] or relativistic quasiparticle time-blocking approximation [5] confirm a neutron surface excitation for 1^- levels with enhanced $B(E1)$ excitation probabilities (e.g., see Refs. [6,7]). However, other mechanisms such as toroidal or compression flows (e.g., see Refs. [8,9]) and clustering effects, here in particular α clusters [10], are also proposed to contribute to low-lying $E1$ strength.

The importance of the low-energy $E1$ strength is manifold. The neutron-skin oscillation picture suggests a separation of proton and neutron matter in the neutron skin. Some theoretical approaches, e.g., Refs. [11–13], show a connection to the symmetry term of the nuclear binding energy and the nuclear equation of state. However, other approaches employing a correlation analysis [14,15] conclude that there is only a marginal correlation between the low-lying $E1$ strength and these quantities. At present, the situation remains controversial. In any case, the presence of additional $E1$ strength near the neutron separation threshold has an impact on neutron-capture rates in astrophysical calculations [16–18]. The 1^- levels forming the PDR have lifetimes in the lower femtosecond or even attosecond range. As a consequence of the associated broad resonance width Γ, these levels act as wide open doorway states in the neutron-capture process. Additionally, the short lifetimes, which approach typical neutron evaporation times, permit a fast depopulation of the capture levels to lower-lying bound states, which stabilizes the newly formed nucleus against subsequent neutron emission. Applying detailed balance, in the photon bath of an astrophysical r-process environment, the PDR levels above the threshold enhance the reverse process of (γ, n) photodissociation. Consequently, for the astrophysical r process that proceeds via neutron-rich nuclei, where the PDR is predicted to be most pronounced, the amount of $E1$ strength and its positioning relative to the neutron separation threshold is of importance.

However, the experimental picture of the $E1$ strength is not consistent. As outlined in Ref. [2], the extracted $E1$ strengths vary significantly depending on the employed experimental technique. At present, the most complete approach is the (p, p') inelastic proton scattering at small

forward angles. This tool allows the extraction of the complete $B(E1)$-excitation strength below and above the neutron threshold [19–21]. However, with respect to theory, the experimental information extracted solely from these experiments is limited to the excitation strength.

A milestone in the experimental investigation of the PDR that allowed an insight into the structure of the wave functions of these 1^- levels, was the comparison of data obtained via the scattering of real photons (γ,γ') and the inelastic scattering of α particles $(\alpha,\alpha'\gamma)$ [6,22–24]. The latter represents an isoscalar probe, which is sensitive to surface excitations and the comparison revealed that the PDR splits into a low-energy isoscalar part and a high-energy isovector part. This feature has been confirmed in (^{17}O, ^{17}O$'\gamma$) scattering; e.g., see Refs. [25,26].

In Ref. [21], a comparison of $^{120}\mathrm{Sn}(p,p')$ and $^{120}\mathrm{Sn}(\gamma,\gamma')$ [27] revealed that the latter technique misses a large fraction of the dipole strength due to unobserved branches. Despite this previously known shortcoming, the (γ,γ') technique, which is commonly denoted as nuclear resonance fluorescence (NRF) [28], is the workhorse for the experimental investigation of the PDR in stable nuclei. The angular-momentum transfer of the (γ,γ') reaction is almost entirely limited to its $1\hbar$ intrinsic angular momentum of the photon and, hence, NRF is sensitive to dipole-excited states and allows the spectroscopy of $J=1$ levels embedded in a sea of levels with other spins. However, the price to pay is that the scattering off the atomic system outweighs the intended scattering off the nucleus by far and the spectra are dominated by this background. Furthermore, for the high-energy γ rays involved, the full-energy detection efficiency, even of modern large volume high-purity germanium detectors, is small, adding incompletely detected events to the atomic background. Consequently, often weak decay branches or even strong decay branches from weakly excited states cannot be resolved from the background. Missing decay branches lead to an underdetermination of the total decay width Γ as well as the ground-state decay width Γ_0 and subsequently to a too low $B(E1)$ strength. Convincing evidence for the nonobservation of such branches in NRF experiments using bremsstrahlung is, for example, presented in Refs. [29,30]. Exploiting NRF with quasimonochromatic Compton-backscattered laser photon beams [31], which excite 1^- levels in a narrow energy range, the observed depopulation of low-lying excited states allowed the extraction of average branching ratios [32–36]. Finally, the total $E1$ strength below the threshold can be extracted but, in terms of a state-by-state spectroscopy, the situation remains unsatisfactory.

An opportunity to obtain these crucial γ-ray branching ratios has recently been highlighted by spectra recorded in total absorption γ-ray spectrometry (TAGS) [37,38] following β decay, which revealed considerable population probabilities for high-lying states. For some β decays such as $^{86}\mathrm{Br}\xrightarrow{\beta}{}^{86}\mathrm{Kr}$, the population of levels with energies corresponding to almost the Q_β value were reported. β decay prefers to connect levels with similar spin and parity and the $J^\pi = 1^-$ ground state of ^{86}Br [39] makes it very likely that, in this particular example, 1^- levels associated with the PDR are populated. This leads to the conclusion that β decays with high Q_β values from mothers with low ground-state spin and negative parity are capable of populating 1^- levels associated with the PDR. In the nuclear landscape a considerable number of such β decays are encountered and examples of such cases are listed in Table I.

TABLE I. Illustrative cases in which β decay can be used to extract information about 1^- levels associated with the pygmy dipole resonance. The spins and parities J^π of the mother nuclei, neutron separation energies S_n, β-decay Q values Q_β, and probability for β-delayed neutron emission $P_{\beta n}$ are taken from the NNDC [39] and XUNDL [40] databases, respectively.

Mother	J^π	Daughter	S_n [keV]	Q_β [keV]	$P_{\beta n}$ [%]
^{48}K	(2^-)	^{48}Ca	9945	12090	1.1
^{50}K	$(0^-,1^-,2^-)$	^{50}Ca	6353	14220	22.5
^{84}Ga	(0^-)	^{84}Ge	5243	12900	42.5
^{86}Br	(1^-)	^{86}Kr	9857	7626	
^{96}Y	0^-	^{96}Zr	7856	7096	
^{98}Y	$(0)^-$	^{98}Zr	6415	8824	0.33
^{130}In	$1^{(-)}$	^{130}Sn	7596	10249	0.92
^{136}I	(1^-)	^{136}Xe	8084	6930	
^{140}Cs	1^-	^{140}Ba	6428	6220	
^{142}Cs	0^-	^{142}Ba	6181	7325	0.09
^{144}Cs	$1^{(-)}$	^{144}Ba	5901	8500	2.9
^{146}Cs	1^-	^{146}Ba	5495	9370	12.4

The aim of this work is to evaluate the extent to which the combination of β decay and (γ,γ') provides improved spectroscopic information and to employ the QPM to investigate the complementary insight into the microscopic structure of the wave function of the 1^- levels of interest provided by β decay. For this purpose the case $^{136}\mathrm{I}\ [J_0=(1^-)] \rightarrow {}^{136}\mathrm{Xe}$ has been chosen as an example. For this decay $Q_\beta = 6.93$ MeV is sufficient to populate higher-lying 1^- levels in a stable nucleus and published data from β-decay studies [41] as well as NRF [42] exist. In the $^{136}\mathrm{Xe}(\gamma,\gamma')$ reaction, large numbers of spin-1 levels were observed below Q_β (see Fig. 3 in Ref. [42]). A comparison of the level populations in both experiments is shown in Fig. 1. It is evident that several levels are observed with both techniques.

At this point it is worth mentioning that the γ rays from the β-decay experiment were recorded using first-generation Ge(Li) semiconductor detectors, each with about 10% γ-ray detection efficiency. None of these detectors was equipped with any type of active anti-Compton shielding. Because of the low γ-ray detection efficiencies in this experiment, $\gamma\gamma$-coincidence events are

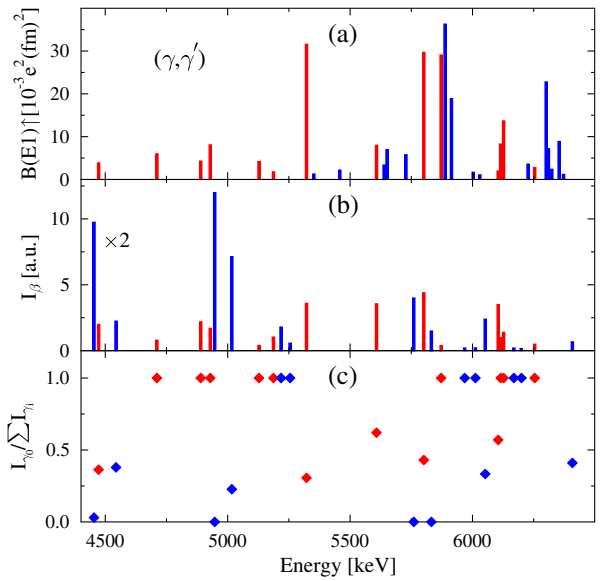

FIG. 1. Candidates for 1^- levels in ^{136}Xe. Part (a) shows the $B(E1)$-strength distribution as extracted from the (γ,γ') reaction [42], part (b) shows the relative level population intensity in the ^{136}I $J^\pi = (1^-)$ β decay [41], and part (c) the ground-state branching ratios extracted from β decay. Levels marked with red bars were populated in both reactions. The $B(E1)$ strengths in part (a) are so far not corrected for the branching ratios from β decay.

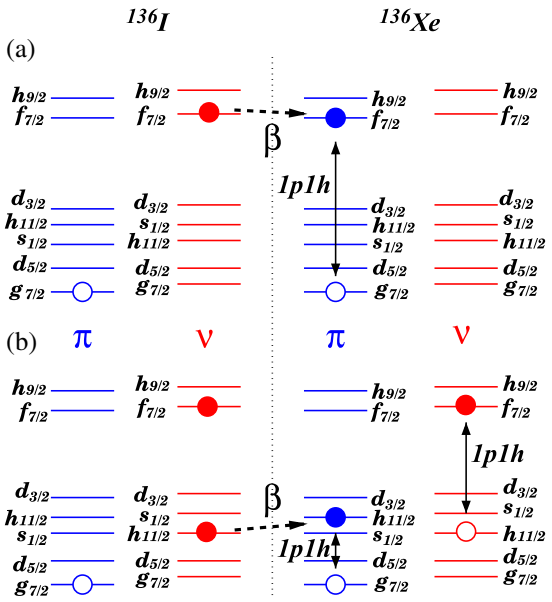

FIG. 2. Schematic picture of ^{136}I β decay. Part (a) shows the population of a $1p1h$ configuration in β decay of a neutron (ν) near the Fermi surface and part (b) shows the population of a $2p2h$ configuration in β decay of a neutron initially situated below the Fermi surface. For simplicity, only unpaired particles (full circles) and holes (empty circles) are presented. For a detailed discussion, see text.

reported only for levels up to an energy of 4.5 MeV. Hence, the assignment of level energies based on γ-ray energies is not unambiguous. Despite this ancient equipment by present standards, the authors performed outstanding work and report γ-ray branches to lower-lying excited states for several levels. Because of the background, none of these branching transitions was resolved in a recent (γ,γ') experiment [42]. However, the (γ,γ') spectra clearly demonstrate that the strong branching transition of the 5322-keV level reported in β decay is, if at all present, much weaker than reported. In Fig. 1 it is also evident that considerable numbers of γ-ray decays were observed exclusively with one of the methods. This observation can have experimental reasons. For example, due to the missing coincidence information in (γ,γ'), only the Ritz combination principle can be used to assign decays to lower-lying excited states. Consequently, some of the γ rays in Fig. 1(a) might correspond to decays to lower-lying excited levels and not to ground-state transitions. Furthermore, levels populated in β decay can have a too small excitation probability in (γ,γ') and are below the sensitivity limit or are subject to the previously mentioned branching ratio problem. In particular, the levels at 4454 and 5016 keV, strongly populated in β decay but not observed in NRF, exhibit large branching transitions to lower-lying exited states. Moreover, in Ref. [42] a negative parity of the observed $J = 1$ levels was assumed, but so far not firmly established. As a result of the parity change, the degree of forbiddenness is higher and the population probability of 1^+ levels is reduced in β decay. Consequently, β-decay data provide valuable additional spectroscopic information, but not for all 1^- levels below Q_β.

A second possibility for the different patterns in Fig. 1 is the role of the populating nuclear reaction. We discuss below the differences in excitation of 1^- states in inelastic particle scattering and NRF experiments with the population of the same set of states in β decay. For simplicity, we restrict the calculations in this initial study to Fermi β decays.

In comparison to ^{136}Xe in its ground state, the nucleus ^{136}I has an extra neutron in the $|f\rangle \equiv |2f_{7/2}\rangle$ level and a proton hole in the $|g\rangle \equiv |1g_{7/2}\rangle$ level which couple to the (1^-) total angular momentum. Theoretically, the ground state of ^{136}I is described as the lowest energy 1^- pn phonon built on top of the ^{136}Xe ground state. The QRPA calculation predicts that this state has an almost pure ($> 99.9\%$) $[\nu f, \pi g^{-1}]_{1^-}$ particle-hole configuration.

If only $1p1h$ excitations in the daughter nucleus are considered, then the Fermi β decay of the neutron in the f level leaves ^{136}Xe in either $[\pi f, \pi g^{-1}]_{1^-}$ [as drawn in Fig. 2(a)] or in the $[\nu f, \nu g^{-1}]_{1^-}$ excited states.

Alternatively, a neutron in some other subshell $|j\rangle$ may also undergo a β decay [e.g., $|j\rangle \equiv |1h_{11/2}\rangle$ in Fig. 2(b)] leaving the daughter nucleus in the $2p2h$ excited state

$[\pi j, \nu f, \pi g^{-1}, \nu j^{-1}]_{1^-}$ [see Fig. 2(b)]. The probability of finding the daughter nucleus in the $^{136}\mathrm{I}\xrightarrow{\beta}{}^{136}\mathrm{Xe}$ reaction in these particular $1p1h$ and $2p2h$ configurations is predicted to be of the same order. The level $|j\rangle$ located between the f and the g levels allows it to have simultaneously a neutron hole and proton particle.

To obtain a more realistic picture of the ^{136}Xe states populated in β decay, it is necessary to project this simple mean-field picture onto more realistic eigen-wave-functions of the final 1^- excited states. The QPM is capable of providing such a set. In Refs. [22,42], there is a good description of the $E1$ fragmentation pattern in ^{136}Xe below the neutron threshold employing wave functions which contain one-, two-, and three-phonon components. The $B(E1)$-strength distribution over this set of states of ^{136}Xe is presented in Fig. 3(a).

For the purpose of this Letter, the QPM was extended to describe the β decay of odd-odd nuclei to excited states of even-even nuclei. Previous β-decay studies [43,44] dealt with even-even mother nuclei.

Within the QPM, the $1p1h$ configurations $[\pi f, \pi 1g^{-1}]_{1^-}$ and $[\nu f, \nu g^{-1}]_{1^-}$ are fragmented over one-phonon 1^-_i states (where $i = 1, 2, \ldots$ is the order number of the phonon with particular λ^π quantum numbers). Analogously, the $2p2h$ $[\pi j, \nu f, \pi g^{-1}, \nu j^{-1}]_{1^-}$ configurations are distributed over two-phonon states with structure $[\lambda_1^{\pi_1} i_1 \times \lambda_2^{\pi_2} i_2]_{1^-}$. The intensity I_β of the population of the QPM states in the $^{136}\mathrm{I}\xrightarrow{\beta}{}^{136}\mathrm{Xe}$ reaction has the form

$$I_\beta = \Bigg| \sum_i \frac{R_i}{\sqrt{8}} [f_f^{(0)} u_f^\pi u_f^\nu X_{fg}^{1^- i}(\pi) - f_g^{(0)} v_g^\pi v_g^\nu X_{fg}^{1^- i}(\nu)] + \sum_{\lambda_1 i_1 \lambda_2 i_2} P_{\lambda_1 i_1}^{\lambda_2 i_2} \frac{\hat{\lambda}_1 \hat{\lambda}_2}{\sqrt{3}} \sum_j \frac{f_j^{(0)} u_j^\pi v_j^\nu}{\hat{j}} \begin{Bmatrix} \frac{7}{2} & \frac{7}{2} & 1 \\ \lambda_1 & \lambda_2 & \mathrm{j} \end{Bmatrix} \times [X_{gj}^{\lambda_1 i_1}(\pi) X_{jf}^{\lambda_2 i_2}(\nu) - X_{fj}^{\lambda_1 i_1}(\nu) X_{jg}^{\lambda_2 i_2}(\pi)] \Bigg|^2, \quad (1)$$

where $f_j^{(0)} = \langle j(p) \| \tau \| j(n) \rangle$ is the reduced matrix element of the Fermi β decay, $\hat{\lambda} = \sqrt{2\lambda + 1}$, u and v are Bogoliubov's coefficients (their squares are the occupation probabilities for holes and particles, respectively), X are the QRPA forward amplitudes, and R and P are the amplitudes of one- and two-phonon components of the QPM wave function, respectively. The calculated intensities I_β are shown in Fig. 3(d).

The intensities of β decays to 1^- states in ^{136}Xe [the first term of Eq. (1)], which are constructed from the $[\nu f, \nu g^{-1}]_{1^-}$ and $[\pi f, \pi g^{-1}]_{1^-}$ $1p1h$ states whose energies are calculated to be 6.9 and 9.7 MeV, respectively, are presented in Fig. 3(e). In fact, only the decays via the neutron component are shown in this figure. The decays via the proton component have excitation energies exceeding

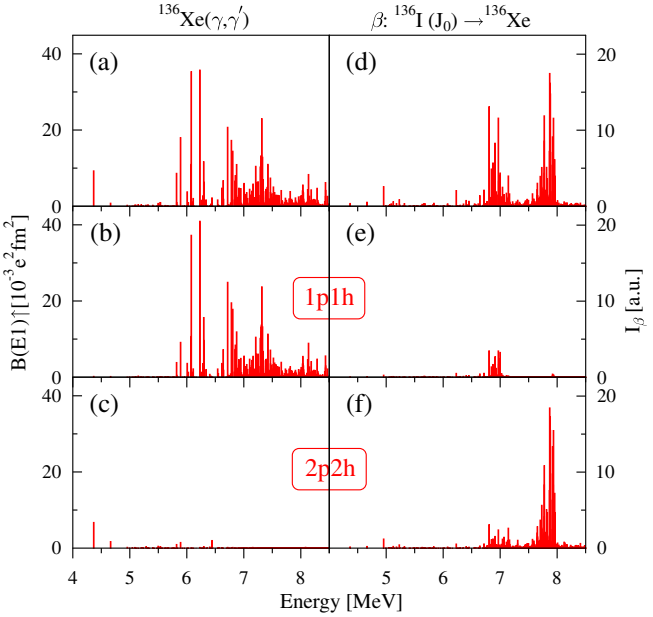

FIG. 3. Comparison of level population of ^{136}Xe in (γ, γ') (a) and β decay (d) of the $^{136}\mathrm{I}(J^\pi = 1^-)$ ground state calculated in the QPM. Panel (b) shows the population of $1p1h$ components in (γ, γ') and panel (e) in β decay. The population of $2p2h$ components in (γ, γ') is shown in panel (c) and for β decay in panel (f). The calculations are elucidated in the text.

8.5 MeV and are not shown in the plot. Figure 3(f) shows the transition intensities predicted by the second term of Eq. (1) corresponding to β decay to two-phonon components of the 1^- state. The sum of the intensities from panels (e) and (f) including the interference between them are plotted in panel (d).

The decays to two-phonon components of 1^- state wave functions is 12.6 times stronger than those to the one-phonon component. This is dramatically different from the case when the 1^- states of ^{136}Xe are excited from the ground state of ^{136}Xe in NRF or when using other inelastically scattered probes. In the latter processes, the excitation proceeds predominantly via the one-phonon components as seen in panels (b) and (c) of Fig. 3. It is worthwhile mentioning that the quantities shown in all six panels of Fig. 3 are plotted for the same set of 1^- states.

Since the QPM often calculates the PDR energy somewhat higher than experiment, the experimental limit of a maximum Q_β value was neglected in the calculations. Consequently, the influence of the phase-space factor for electrons and antineutrinos on the level population probability is so far not implemented. Nevertheless, the comparison of the distinct level population properties calculated within the QPM (Fig. 3) allows, when applied to the experimental data shown in Fig. 1, conclusions to be drawn about the structure of the observed levels. For example, the calculations predict that the states with a strong $[\nu f_{7/2}, \nu g_{7/2}^{-1}]$ configuration in their wave function should

be well excited in both reactions. The experimentally observed levels at 5322, 5801, and 5872 keV exhibit this feature. The levels strongly excited in NRF but not populated in β decay are probably dominated by other neutron configurations such as, for example, $[\nu 1i_{13/2}, \nu 1h^{-1}_{11/2}]$ or $[\nu 3p_{3/2}, \nu 2d^{-1}_{5/2}]$. At the same time, the levels at 4454 and 5016 keV observed in β decay only are good candidates to be two-phonon states. This statement is also supported by their weak decay to the ground state. The observation that the energy of levels containing a strong $[\nu f_{7/2}, \nu g^{-1}_{7/2}]$ $1p1h$ component is lower than the calculated two-quasiparticle configuration indicates that its energy needs refinement. Hence, the new spectroscopic information provides a new test for the model.

In this Letter, shortcomings of the PDR studies in inelastic scattering experiments are discussed. It is demonstrated that β decay populates levels associated with the PDR, but only a fraction of those. Spectroscopy following β decay, with its comparably background-free spectra and opportunity to perform $\gamma\gamma$-coincidence measurements, will supplement other experimental techniques such as NRF or possibly even relativistic Coulomb excitation (e.g., see Ref. [45]). The QPM calculations demonstrate that the comparison of level-population probabilities provide an alternative insight into the microscopic structure of the wave functions of 1^- levels. Hence, β decay represents an additional probe for PDR studies.

The authors appreciate valuable discussion with A. P. Tonchev and K. Rykaczewski. Support from STFC and SUPA is acknowledged by M. S., L. P. G., E. T. G., and P. S. V. P. and N. P. gratefully acknowledge the financial support of the DFG under Grant No. SFB-1245.

*marcus.scheck@uws.ac.uk

[1] M. Harakeh and A. van der Woude, *Giant Resonances* (Oxford University Press, Oxford, 2001).
[2] D. Savran, T. Aumann, and A. Zilges, Prog. Part. Nucl. Phys. **70**, 210 (2013).
[3] N. Paar, D. Vretenar, E. Khan, and G. Colò, Rep. Prog. Phys. **70**, 691 (2007).
[4] V. G. Soloviev, *Theory of Atomic Nuclei, Quasiparticles and Phonons* (IOP, London, 1992).
[5] E. Litvinova, P. Ring, and V. Tselyaev, Phys. Rev. C **78**, 014312 (2008).
[6] J. Endres *et al.*, Phys. Rev. Lett. **105**, 212503 (2010).
[7] E. G. Lanza, A. Vitturi, and M. V. Andrés, Phys. Rev. C **91**, 054607 (2015).
[8] A. Repko, P.-G. Reinhard, V. O. Nesterenko, and J. Kvasil, Phys. Rev. C **87**, 024305 (2013).
[9] P.-G. Reinhard, V. O. Nesterenko, A. Repko, and J. Kvasil, Phys. Rev. C **89**, 024321 (2014).
[10] M. Spieker, S. Pascu, A. Zilges, and F. Iachello, Phys. Rev. Lett. **114**, 192504 (2015).
[11] J. Piekarewicz, Phys. Rev. C **73**, 044325 (2006).
[12] J. Piekarewicz, Phys. Rev. C **83**, 034319 (2011).
[13] N. Paar, Ch. C. Moustakidis, T. Marketin, D. Vretenar, and G. A. Lalazissis, Phys. Rev. C **90**, 011304(R) (2014).
[14] P.-G. Reinhard and W. Nazarewicz, Phys. Rev. C **81**, 051303 (2010).
[15] P.-G. Reinhard and W. Nazarewicz, Phys. Rev. C **87**, 014324 (2013).
[16] S. Goriely, Phys. Lett. B **436**, 10 (1998).
[17] S. Goriely, E. Khan, and M. Samyn, Nucl. Phys. **A739**, 331 (2004).
[18] N. Tsoneva, S. Goriely, H. Lenske, and R. Schwengner, Phys. Rev. C **91**, 044318 (2015).
[19] A. Tamii *et al.*, Phys. Rev. Lett. **107**, 062502 (2011).
[20] I. Poltoratska *et al.*, Phys. Rev. C **85**, 041304 (2012).
[21] A. M. Krumbholz *et al.*, Phys. Lett. B **744**, 7 (2015).
[22] D. Savran, M. Babilon, A. M. van den Berg, M. N. Harakeh, J. Hasper, A. Matic, H. J. Wörtche, and A. Zilges, Phys. Rev. Lett. **97**, 172502 (2006).
[23] J. Endres, D. Savran, A. M. van den Berg, P. Dendooven, M. Fritzsche, M. N. Harakeh, J. Hasper, H. J. Wörtche, and A. Zilges, Phys. Rev. C **80**, 034302 (2009).
[24] V. Derya *et al.*, Phys. Lett. B **730**, 288 (2014).
[25] A. Bracco, F. C. L. Crespi, and E. G. Lanzaand, Eur. Phys. J. **A51**, 99 (2015).
[26] F. C. L. Crespi *et al.*, Phys. Rev. C **91**, 024323 (2015).
[27] B. Özel-Tashenov *et al.*, Phys. Rev. C **90**, 024304 (2014).
[28] U. Kneissl, H. H. Pitz, and A. Zilges, Prog. Part. Nucl. Phys. **37**, 349 (1996).
[29] F. Bauwens, J. Bryssinck, D. De Frenne, K. Govaert, L. Govor, M. Hagemann, J. Heyse, E. Jacobs, W. Mondelaers, and V. Yu. Ponomarev, Phys. Rev. C **62**, 024302 (2000).
[30] M. Scheck *et al.*, Phys. Rev. C **88**, 044304 (2013).
[31] N. Pietralla *et al.*, Phys. Rev. Lett. **88**, 012502 (2001).
[32] A. P. Tonchev, S. L. Hammond, J. H. Kelley, E. Kwan, H. Lenske, G. Rusev, W. Tornow, and N. Tsoneva, Phys. Rev. Lett. **104**, 072501 (2010).
[33] C. T. Angell, S. L. Hammond, H. J. Karwowski, J. H. Kelley, M. Krtička, E. Kwan, A. Makinaga, and G. Rusev, Phys. Rev. C **86**, 051302 (2012).
[34] M. Scheck *et al.*, Phys. Rev. C **87**, 051304(R) (2013).
[35] J. Isaak *et al.*, Phys. Lett. B **727**, 361 (2013).
[36] C. Romig *et al.*, Phys. Rev. C **88**, 044331 (2013).
[37] A. Fijałkowska *et al.*, Acta Phys. Pol. B **45**, 545 (2014).
[38] J. L. Tain *et al.*, Phys. Rev. Lett. **115**, 062502 (2015).
[39] http://www.nndc.bnl.gov/endsf.
[40] http://www.nndc.bnl.gov/xundl.
[41] W. R. Western, J. C. Hill, W. L. Talbert, and W. C. Schick, Phys. Rev. C **15**, 1822 (1977).
[42] D. Savran *et al.*, Phys. Rev. C **84**, 024326 (2011).
[43] V. A. Kuzmin and V. G. Soloviev, J. Phys. G **10**, 1507 (1984).
[44] A. P. Severyukhin, V. V. Voronov, I. N. Borzov, N. N. Arsenyev, and N. Van Giai, Phys. Rev. C **90**, 044320 (2014).
[45] P. Adrich *et al.*, Phys. Rev. Lett. **95**, 132501 (2005).